Experimental Verification of Noise Induced Attractor Deformation

Martin Diestelhorst,[1] Rainer Hegger,[2] Lars Jaeger,[2,*] Holger Kantz,[2] and Ralf-Peter Kapsch[1,2]
[1]*Fachbereich Physik, Martin-Luther-Universität Halle-Wittenberg, Friedemann-Bach-Platz 6, 06108 Halle, Germany*
[2]*Max-Planck-Institut für Physik komplexer Systeme, Nöthnitzer Strasse 38, D-01187 Dresden, Germany*
(Received 29 October 1998)

A periodically driven nonlinear electric resonance circuit with a ferroelectric inside the capacitance shows the recently discovered effect of noise induced attractor deformations. By exposing the system to dynamical noise we observe and quantitatively characterize the effect of attractor elongation due to perturbations at homoclinic tangencies. The analysis of the experimental observations fits perfectly with theoretical predictions. [S0031-9007(99)08661-5]

PACS numbers: 05.45.Ac, 05.40.Ca, 07.50.Ek

Noise is ubiquitous in experiments and even, by noiselike round-off errors, in numerical simulations. Since infinitesimal perturbations are known to grow exponentially fast in deterministic chaotic systems, noise interfering with the dynamics (*dynamical noise*) can be of considerable relevance in real systems. Thus the pioneering works on chaos in deterministic systems were soon followed by research on the interaction between nonlinear dynamics and stochastic processes. One relevant result is given by the shadowing lemma of Bowen [1] and Anosov [1]: In hyperbolic systems, in the vicinity of each pseudoorbit generated by permanently perturbing the system's state there is a solution of the unperturbed system (shadowing). The distance between this solution and the pseudoorbit can be interpreted as measurement noise. Thus if the purely deterministic system creates a fractal attractor, this fractality is smeared out on scales below the noise level, but the attractor remains unchanged on length scales larger than the noise level. Hyperbolicity is given, when at each point on the attractor the tangent space can be uniquely decomposed into stable and unstable subspaces and when these are everywhere transverse to each other. However, almost all known model equations which can be related to realistic physical systems are nonhyperbolic, so that this theorem does not apply. Recently, it was observed that different kinds of nonhyperbolicity, among them that introduced through homoclinic tangencies, does in fact destroy shadowability [2–4].

Homoclinic tangencies are points on the attractor, where the stable and unstable manifolds are tangential to each other. Thus they do not span the tangent space, and perturbations transverse to these manifolds do neither grow nor shrink exponentially but are subject to effects related to the local structure in space. This is visualized in Fig. 1: Since distances along the attractor (which coincides with the unstable manifold) grow under forward iteration but shrink along the stable manifold, the local curvature at a homoclinic tangency diverges under forward iteration [5]. A continuation of this structure into the vicinity of the attractor using the concept of the unstable foliation shows that at these points perturbations can be amplified (by factors of 5 or more in typical maps). Thus the attractor of the system subject to dynamical noise is deformed at certain homoclinic tangencies (noise induced attractor deformation) [2].

In short, the predictions of the theory are the following: Dynamical noise leads to a fattening of the whole attractor at every point, and this is of the order of the noise level. At the images of certain homoclinic tangencies, namely, those where the sum of the curvatures of stable and unstable manifold is minimal and which are called primary [5,6], an elongation of the attractor occurs. This elongation is proportional to the noise level (at least for maps with an almost one-dimensional attractor; for a recent generalization, see [4]), and the proportionality factor increases monotonically with the number of iterates from the primary tangency. The primary homoclinic tangencies are marked by a kind of symmetry under time reversal: Perturbations at a primary tangency are amplified both

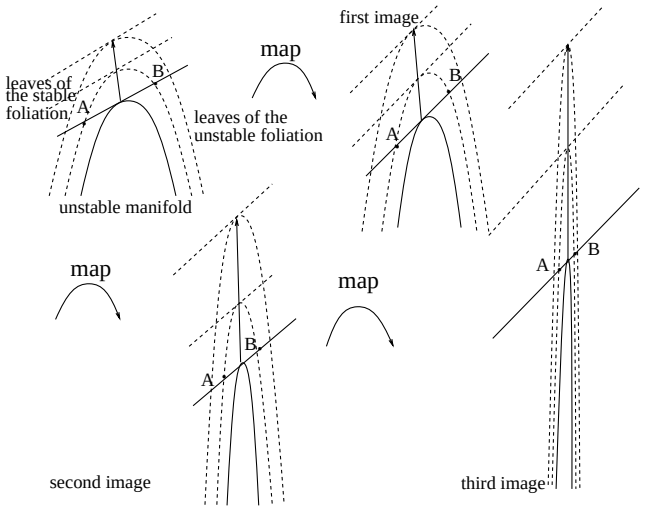

FIG. 1. Structure of the stable and unstable foliation at a homoclinic tangency and its images: The points *A* and *B* are attracted towards each other along the stable manifold; they repel each other along the arc of the unstable direction. A perturbation (the arrow) is thus stretched and moved away from the attractor (continuous line) (figure taken from [2]).

 0031-9007/99/82(11)/2274(4)$15.00

under forward and backward iteration. This property will be exploited below to identify the primary tangencies numerically and is in fact a much better criterion than the one used previously, interpreting the curvatures.

The locations of attractor elongation can be predicted experimentally by the superposition of attractors for slightly different parameter values, since parts of the attractor where the noise induced elongations occur are also those where parameter changes modify the attractor most dramatically. This reflects the fact that nonhyperbolicity also destroys structural stability, i.e., the possibility to counterbalance parameter changes by a change of coordinates [7].

The experiment [8] was performed at an electric series resonance circuit, consisting of a linear inductance of $L = 100$ mH and a nonlinear capacitance C_{nl} formed by a thin plate of ferroelectric Triglycine sulfate (TGS), with 7.31×4.66 mm^2 electroded area and 0.28 mm thick. The temperature of the TGS capacitor was $T = 308$ K, i.e., below the phase transition temperature of $T_c = 322$ K. The circuit was driven by a sinusoidal voltage of 14.04 V_{rms} and a frequency of 2369 Hz, so that switching of the ferroelectric domains occurred. Under certain simplifying assumptions one can derive a damped and driven Duffing equation as a model for the dynamics [9]. Although the formation of domains inside the TGS and possible relaxation phenomena violate these assumptions, there is very good evidence that a second order ordinary differential equation with a periodic driving term is capable of a full description of the observed dynamics [10]. Thus a stroboscopic view of the experimental data represents a two-dimensional section through the three-dimensional phase space of the system without any projection.

In the experiment, the dielectric displacement D at the capacitance and its temporal derivative $\dot{D}$ through the circuit were measured by the voltages across a large linear capacitance (for D) and a small resistance (for $\dot{D}$) in series with the circuit (see Fig. 2 and Ref. [10]).

Sampling both signals exactly with the driving frequency of the sinusoidal voltage using the external clock mode of the digital oscilloscope Nicolet Pro30 and the synchronous output signal of a function generator HP33120A, which is phase locked with the driving generator HP3325B, stroboscopic sections of the attractor were recorded. Phase locking and tuning the phase between driving voltage and the synchronous signal of the HP33120A allowed the observation of different stroboscopic sections of the same attractor. So it was possible to look experimentally for the most promising Poincaré sections, where a slight increase of the magnitude of the driving voltage caused the largest elongation of the attractor. Stochastic noises of adjustable amplitudes and almost uniform distribution, generated by a second HP33120A generator, were added to the driving voltage and thus coupled into the system. In Fig. 3 we show a series of stroboscopic views with increasing noise levels. The effect

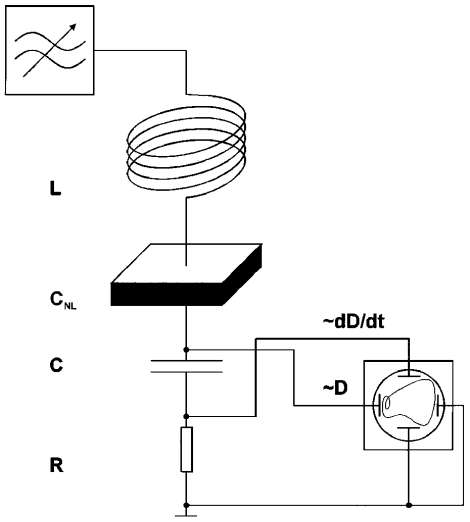

FIG. 2. The nonlinear series resonance circuit including the elements for measuring the dielectric displacement D and its temporal derivative $\dot{D}$.

of noise induced attractor deformation can be clearly seen in the left parts of the attractor: The attractor is stretched more than it is fattened. For large noise levels, these elongations are curved, merging for even more noise.

In Fig. 4 we show the elongation of these two arms (extracted from plots of the attractors) as a function of the noise amplitude. The result is in agreement with the predicted proportionality between elongation and noise level. The factor of proportionality will be called stretching factor in the following. For large noise amplitudes rather large errors are induced by the finite number of points representing quite thin tails, which is taken into account by the error bars. The lowest curve shows the "fattening" of the attractor due to noise and thus a kind of effective noise level. The upper left arm of the attractor grows with a stretching factor of 5.5 (central curve) and the lower left with a factor of 7 (upper curve) faster than the attractor gets fatter.

In the stroboscopic view, our data represent a two-dimensional map. We can approximate the dynamics by local linear models [11]

$$\vec{x}_{n+1} = \mathbf{A}_n \vec{x}_n + \vec{b}_n \,, \tag{1}$$

where $\mathbf{A}_n$ and $\vec{b}_n$ are designed to minimize the one-step prediction error

$$s_n^2 = \sum_{k:\vec{x}_k \in \mathcal{U}_n} (\vec{x}_{k+1} - \mathbf{A}_n \vec{x}_k + \vec{b}_n)^2 \tag{2}$$

computed for a small neighborhood $\mathcal{U}_n$ of $\vec{x}_n$. The matrices $\mathbf{A}_n$ are identical to the Jacobians at $\vec{x}_n$ of the stroboscopic map. Define $\vec{e}^{\,+}$ to be the eigenvector of the smallest eigenvalue of $\mathbf{C}_f = (\prod_{k=n-l}^{n} \mathbf{A}_k)^\dagger (\prod_{k=n-l}^{n} \mathbf{A}_k)$ and $\vec{e}^{\,-}$ to be the eigenvector of the smallest eigenvalue of $\mathbf{C}_b = (\prod_{k=n+l}^{n} \mathbf{A}_k^{-1})^\dagger (\prod_{k=n+l}^{n} \mathbf{A}_k^{-1})$ (i.e., backward

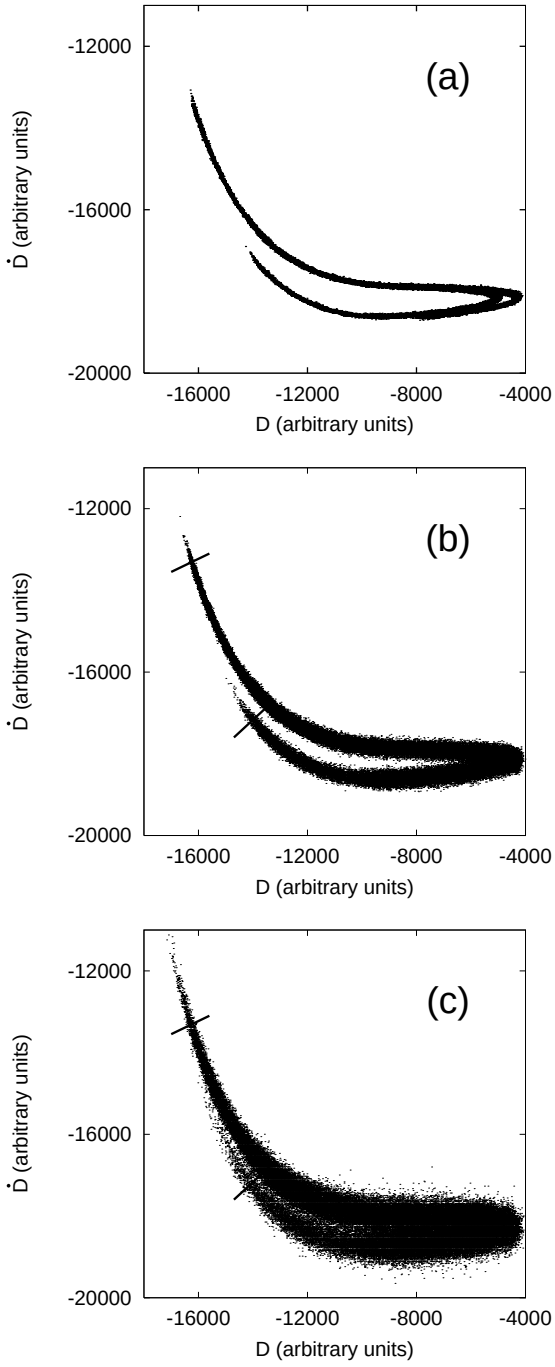

FIG. 3. Stroboscopic views of the experimental data: Noise-free (a), 3% (b), and 6% (c) of noise coupled into the dynamics. Noise level in the root mean square sense in relation to the amplitude of the driving voltage. The bars perpendicular to the attractor denote the left endings of the unperturbed attractor.

iteration of the inverse Jacobians). As discussed in [2], $\vec{e}^{+}$ converges fast (in l) towards the tangent of the stable manifold at $\vec{x}_n$, whereas $\vec{e}^{-}$ converges towards the tangent of the unstable manifold in $\vec{x}_n$. At a homoclinic tangency both vectors are parallel, or, in other words, the most expanding direction of $\prod_{k=n-l}^{n} \mathbf{A}_k$ is perpendicular to the attractor. At these points, the largest eigenvalues

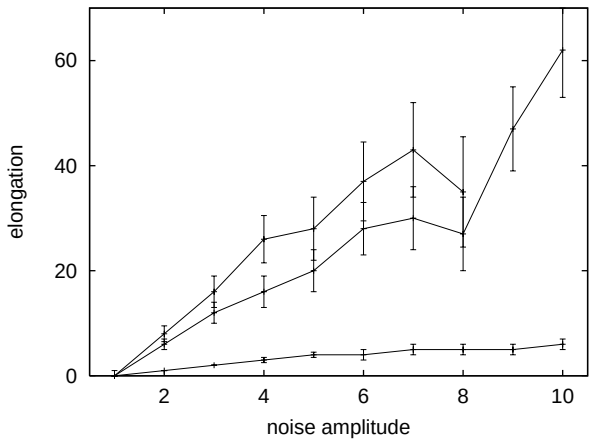

FIG. 4. The elongation (in arbitrary units) of the two left parts of the attractor (with respect to the unperturbed attractor shown in Fig. 3a) and its fattening as a function of the noise amplitude in percent of the driving voltage (curves from top to bottom: lower left arm, upper left arm, fattening).

of $\mathbf{C}_f$ and $\mathbf{C}_b$ give the squares of the expansion rates of perturbations off the attractor under forward and backward iteration, respectively. They allow one to characterize whether a homoclinc tangency is primary, a preimage, or an image, and the largest eigenvalue of $\mathbf{C}_f$ predicts (if an image) the noise amplification. Primary tangencies are characterized by the fact that the stretching factor is larger than unity both forward and backward in time, whereas for nonprimary tangencies it is either forward larger and backward smaller than unity (images of the primary tangency) or forward smaller and backward larger than unity (preimages).

In Fig. 5 we show again the experimental stroboscopic view of the noiseless attractor together with different candidates for homoclinic tangencies obtained from the experimental data. For each point of the time series we computed $\vec{e}^{+}$ and $\vec{e}^{-}$ and plotted a filled circle when the angle between them is smaller than $\pi/100$ and if they

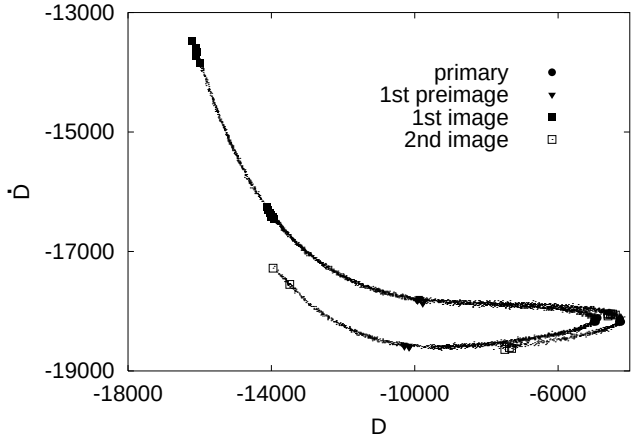

FIG. 5. The attractor together with the numerically determined homoclinic tangencies.

simultaneously fulfill the condition to be primary, i.e., when both stretching factors are larger than unity. We include their two images and one preimage, which by construction are also (close to) homoclinic tangencies. In this way the information about the dynamics in tangent space of the noiseless data yields stretching factors of 6 for the upper and 7.2 for the lower arm. This is in reasonable agreement with the values 5.5 and 7 which we extract visually from the noisy attractors and are reported in Fig. 4.

These results prove that the noise amplification does occur at homoclinic tangencies, it does occur at the first and second images of the primary tangencies, and there is no amplification at the primary tangencies or its preimages. Moreover, we do not find any more positions where noise induced attractor deformation should occur, since the next images of the homoclinic tangencies are all located inside the attractor. This is a result of strong folding: In a noiseless representation we expect to see a fractal structure with more arms, but these arms are extremely close to the prominent lower part of the attractor and cannot be resolved any more. For large noise levels, also the lower arm merges with the upper one, making it impossible to estimate its length any more (reason for the truncation of the upper curve in Fig. 4).

To summarize, it is shown that nonhyperbolicity has effects that are experimentally verifiable. Certain loci of nonhyperbolic structure, the images of primary homoclinic tangencies, give rise to elongations of the attractor when the deterministic dynamics is perturbed by noise. Moreover, the theoretical concept of "primary homoclinic tangency" becomes relevant for the interpretation of the experimental findings, since without this concept (and the theory behind it) one could not understand why the right parts of the attractor are not elongated. In [4] a scaling law $\delta_{\max} \simeq \epsilon^{1/D_1}$ was derived. In this law, δ corresponds to what we call elongation, ϵ is the noise amplitude, and D_1 is the information dimension of the attractor. Our Fig. 4 suggests the validity of this law with $D_1 \approx 1$, which is in agreement with the fact that the flow attractor is close to two dimensional and thus the stroboscopic attractor is almost one dimensional.

*Present address: Olsen & Associates, Zürich, Switzerland.

[1] B. V. Anosov, Proc. Steklov Inst. Math. **90**, 1 (1967); R. Bowen, J. Differential Equations **18**, 333 (1975).
[2] L. Jaeger and H. Kantz, Physica (Amsterdam) **105D**, 79–96 (1997).
[3] C. Grebogi, S. M. Hammel, J. Yorke, and T. Sauer, Phys. Rev. Lett. **65**, 1527 (1990); S. Dawson, C. Grebogi, T. Sauer, and J. A. Yorke, Phys. Rev. Lett. **73**, 1927 (1994).
[4] C. G. Schroer, E. Ott, and J. A. Yorke, Phys. Rev. Lett. **81**, 1397–1400 (1998).
[5] F. Giovannini and A. Politi, J. Phys. A **24**, 1837 (1991).
[6] P. Grassberger and H. Kantz, Phys. Lett. **113A**, 235 (1985).
[7] For example, J. Guckenheimer and P. Holmes, *Nonlinear Oscillations, Dynamical Systems, and Bifurcation of Vector Fields* (Springer, New York, 1983).
[8] M. Diestelhorst and H. Beige, Ferroelectrics **81**, 15 (1988); E. Brauer, H. Beige, L. Flepp, and M. Klee, Phase Transitions **42**, 167 (1993).
[9] H. Beige, M. Diestelhorst, R. Forster, and T. Krietsch, Phase Transitions **37**, 312 (1992).
[10] R. Hegger, H. Kantz, F. Schmüser, M. Diestelhorst, R.-P. Kapsch, and H. Beige, Chaos **8**, 727–736 (1998).
[11] For example, J. D. Farmer and J. J. Sidorowich, Phys. Rev. Lett. **59**, 845 (1987); J. P. Crutchfield and B. S. McNamara, Complex Systems **1**, 417 (1987).